Study of Shock Tube Problem on Two-dimensional Triangular Grids by means of RoeVLPA Scheme

Phongthanapanich S.

Department of Mechanical Engineering Technology, College of Industrial Technology, King Mongkut's University of Technology North Bangkok, Bangkok 10800, Thailand
E-mail address: sutthisakp@kmutnb.ac.th

Abstract

A Roe flux-difference splitting scheme with an entropy and shock fixes (RoeVLPA) for high-speed compressible flow analysis on structured triangular grid is presented. The proposed method heals nonphysical flow solutions such as the carbuncle phenomenon, the shock instability from the odd-even decoupling problem, and the expansion shock generated from the violated entropy condition. The proposed scheme is further extended to obtain higher-order spatial and temporal solution accuracy. A computational model of a shock tube being used in laboratory is presents to investigate the characteristics of the shock wave. The performance and efficiency of the proposed method are evaluated by solving several shock tube problems.

Keywords*: Shock instability, entropy fix, Explicit scheme, Shock tube problem, Roe FDS scheme*

1 Introduction

In general all fluids are naturally compressible but they are categorized into compressible and incompressible fluids, depending on their degree of compressibility. A fluid whose density varies in an appreciable amount under high pressure load is called a compressible fluid, and the main difference between compressible and incompressible fluids is the rate at which forces are transmitted through the fluid itself [1]. Currently, compressible flows including shock waves are present in numerous situations. Then the problem of a fixed shock in a steady flow can simply be modelled and the solution consists in the Rankine-Hugoniot relationships. A pressure disturbance transmits in the form of successive compression and rarefaction waves due to its elastic in nature. This pressure disturbance is called a finite disturbance when a perturbation in the thermodynamic state of quiescent gas causes variations in pressure and density the same order as that of values of pressure and density. When the strength of a disturbance becomes large enough, the speed of the wave may increases beyond the speed of a sound wave, and this generated wave of higher amplitude is called a shock wave.

A shock tube is equipment for generating gas flows of very short duration, and commonly used to generate shock or blast waves in the laboratory. It consists of a tube of constant cross section in which a diaphragm initially separates two bodies of gas at different pressures. Rapid removal of the diaphragm generates a flow of short duration containing waves of finite amplitude separated by quasi-steady regions. Initially, a shock wave travels into the low pressure gas while an expansion or rarefaction wave travels into the high pressure gas. The quasi-steady flow regions induced behind these waves are separated by a contact surface across which pressure and velocity are equal.

During the past decades, a variety of shock-capturing schemes have been developed for solving the Euler equations of gas dynamics. The Godunov method has been widely used and shown to produce high precision for simulations of complex shock phenomena. However, the method has some weakness and may fail or produce physically unrealistic numerical solutions for some problems. These problems include the high Mach number flow past a blunt body [2], and the moving shock in a straight duct from an odd-even grid perturbation [3]. Similar to the Godunov method, the original Roe scheme [4] has been widely employed and applied to solve complex flow problems. The scheme was also found to produce physically unrealistic expansion shock for flow over a forward facing step because it does not satisfy the entropy condition [5]. Some numerical experiments have shown that the extension of the one-dimensional upwind scheme to multidimensional problems often yields poor stationary shock at high Mach number aligned with the structured mesh. To overcome this problem, [5-10] proposed the entropy fix formulation to replace the near zero eigenvalues by some tolerances.

The main objective of this paper is to study shock tube problem by using a Roe flux-difference splitting scheme with an entropy and shock fixes (RoeVLPA) [9] on two-dimensional structured triangular grids. The entropy and shock fix methods [4,6] are modified herein for triangular mesh and implemented into the original Roe scheme so called RoeVLPA scheme. The presentation in this paper starts from Section 2 describing the Euler equations used in the analysis of high-speed compressible flows and the solution procedure that lead to the computer program development. Then the Roe scheme with entropy and shock fix methods is then presented. Finally, the proposed method is further extended to achieve higher-order solution accuracy and then evaluated by several benchmark test cases in Section 3 for solving several shock tube problems.

2 Roe scheme with entropy and shock fixes formulation

The governing differential equations of the Euler equations for the two-dimensional inviscid flow are given by,

$$\frac{\partial \boldsymbol{U}}{\partial t}+\frac{\partial \boldsymbol{E}}{\partial x}+\frac{\partial \boldsymbol{G}}{\partial y}=0 \tag{1}$$

where $\boldsymbol{U}$ is the vector of conservation variables, $\boldsymbol{E}$ and $\boldsymbol{G}$ are the vectors of the convection fluxes in x and y directions, respectively. The perfect gas equation of state is in the form,

$$p=\rho e(\gamma-1) \tag{2}$$

where p is the pressure, ρ is the density, e is the internal energy, and γ is the specific heat ratio (1.4 for air).

By integrating Eq. (1) over a control volume, Ω, and applying the divergence theorem to the resulting flux integral,

$$\frac{\partial}{\partial t}\int_{\Omega}\boldsymbol{U}d\Omega+\int_{\partial\Omega}\boldsymbol{F}\cdot\hat{\boldsymbol{n}}dS=0 \tag{3}$$

where $\boldsymbol{F}$ is the numerical flux vector and $\hat{\boldsymbol{n}}$ is the normal unit vector to the cell boundary. The numerical flux vector at the cell interface between the left cell L and the right cell R according to the Roe scheme [4] is written as

$$\boldsymbol{F}_n=\frac{1}{2}(\boldsymbol{F}_{nL}+\boldsymbol{F}_{nR})-\frac{1}{2}\sum_{k=1}^{4}\alpha_k|\lambda_k|\boldsymbol{r}_k \tag{4}$$

where $\lambda_k=\lfloor V_n-a \quad V_n \quad V_n \quad V_n+a\rfloor^T$, α_k is the wave strength of the k^{th} wave, $\boldsymbol{r}_k$ is the corresponding right eigenvector, V_n is the normal velocity, and a is the speed of sound at the cell interface.

This paper proposes a Roe with entropy and shock fixes (RoeVLPA) that combines the entropy fix methods of Van Leer *et al*. [6] and Pandolfi and D'Ambrosio [5] by modifying the original eigenvalues as follows:

$$|\lambda_k|=\begin{cases}|\lambda_{1,4}| & ,|\lambda_{1,4}|\geq 2\eta^{VL}\\ \dfrac{|\lambda_{1,4}|^2}{4\eta^{VL}}+\eta^{VL} & ,|\lambda_{1,4}|<2\eta^{VL}\\ \kappa\max\left(|\lambda_{2,3}|,\eta^{PA}\right) & \end{cases} \tag{5}$$

where

$$\eta^{VL}=\max(\lambda_R-\lambda_L,0) \tag{6}$$

$$\eta^{PA}=\max(\eta_2,\eta_3,\eta_4,\eta_5) \tag{7}$$

The constant value κ is usually less than or equal to one for the first-order scheme and more than one for higher-order scheme. After performing the numerical experiment, the value of κ is problem dependent in case of the higher-order scheme. An appropriate range of κ for the higher-order scheme is between 1.5 and 6.5, with the recommended value of 2. The sensitivity of the value of κ to the density and pressure perturbations for the odd-even decoupling problem is investigated [9], where the higher values of κ yields more damping rate for the density and pressure perturbations. Thus for simplicity, the value of κ is taken to be one throughout this paper, or otherwise a certain value is specified when appropriate.

3 High-order Numerical Scheme

Solution accuracy from the first-order formulation described in the preceding sections can be improved by implementing a high-order formulation for both the space and time. A high-order spatial discretization is achieved by applying the Taylor' series expansion to the cell-centered solution for each cell face [11], and can be reconstructed from,

$$\boldsymbol{q}_{face} = \boldsymbol{q}_{centroid} + \psi \nabla \boldsymbol{q} \cdot \boldsymbol{r} \tag{8}$$

where $\boldsymbol{q} = [\rho \quad u \quad v \quad p]^T$ consists of the primitive variables of the density, the velocity components, and the pressure, respectively; $\nabla \boldsymbol{q}$ represents the gradient of the variables, and $\boldsymbol{r}$ is the vector projected to the given cell face. The ψ in Eq. (8) represents the limiter, preventing spurious oscillation that may occur in the region of high gradients. In this study, Vekatakrishnan's limiter function [12] is selected,

$$\Psi_C = \min_{i=1,2,3} \begin{cases} \phi\left(\dfrac{\Delta_{+,\max}}{\Delta_-}\right) & , \Delta_- \geq 0 \\ \phi\left(\dfrac{\Delta_{+,\min}}{\Delta_-}\right) & , \Delta_- < 0 \\ 1 & , \Delta_- = 0 \end{cases} \tag{9}$$

where $\Delta_- = \boldsymbol{q}_c - \boldsymbol{q}_i$, $\Delta_{+,\max} = \boldsymbol{q}_{\max} - \boldsymbol{q}_i$, and $\Delta_{+,\min} = \boldsymbol{q}_{\min} - \boldsymbol{q}_i$. The $\boldsymbol{q}_{\max}$ and $\boldsymbol{q}_{\min}$ are respectively the maximum and minimum values of all distance-one neighboring cells. The function ϕ is expressed in the form,

$$\phi(y) = \frac{y^2 + 2y}{y^2 + y + 2} \tag{10}$$

And the second-order temporal accuracy is achieved by implementing the second-order accurate Runge-Kutta time stepping method [13],

$$\begin{aligned} \boldsymbol{U}_i^* &= \boldsymbol{U}_i^n - \frac{\Delta t}{\Omega_i} \sum_{j=1}^{3} \boldsymbol{F}^n \cdot \boldsymbol{n}_j \\ \boldsymbol{U}_i^{n+1} &= \frac{1}{2}\left[\boldsymbol{U}_i^0 + \boldsymbol{U}_i^* - \frac{\Delta t}{\Omega_i} \sum_{j=1}^{3} \boldsymbol{F}^* \cdot \boldsymbol{n}_j\right] \end{aligned} \tag{11}$$

where Δt is the time step.

4 Shock Tube Problem Results

The high-order extension of the RoeVLPA scheme presented in the preceding section is evaluated by solving several shock tube problems. From the solution of Riemann problems one finds directly how much velocity, density, and pressure flows into a cell from the interface under consideration. This section shows simulation of gas dynamic problems to study the effects of Riemann problems on the physical properties for the perfect gas. These selected test cases are: (1) Sod shock tube, (2) Strong shock problem, and (3) Symmetric rarefaction wave problem.

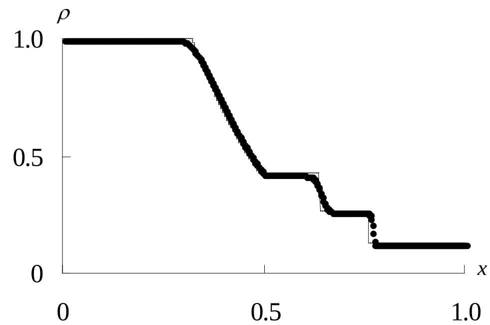

(a) $O(1)$ of density

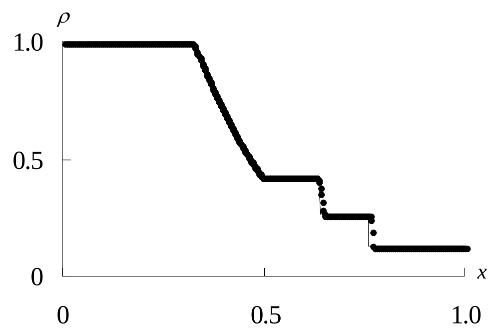

(b) $O(2)$ of density

Figure 1: Comparision of exact and numerical solutions of density.

4.1 *Sod shock tube*

The one-dimensional shock tube test case, the so called Sod shock tube [14], is solved by using a two-dimensional domain. The Sod shock tube is a Riemann problem used as a standard test problem. The initial conditions of the fluids on the left and right sides are given by $(\rho, u, p)_L = (1,0,1)$ and

$(\rho,u,p)_R = (0.125,0,0.1)$. The 1×0.1 computational domain is discretized with uniform triangular elements into 400 and 40 equal intervals in the *x* and *y* directions, respectively. Figures 1(a)-(b) to 3(a)-(b) show the numerical density, pressure, and *x*-velocity distributions along the tube length and are compared with the exact solutions at time $t = 0.15$. The figures show that the rarefaction wave is moving to the left.

The solution is continuous in this region but some of the derivatives of the fluid quantities may not be continuous. The shock wave is moving to the right, and across a shock all quantities will in general be discontinuous. The discontinuous between a shock and a tail of rarefaction wave as shown in Figures 1(a)-(b) is called a contact discontinuity. The figures show that the contact surface is spread out due to the numerical viscosity of the numerical scheme. Finally, the figures show that the high-order extension of the RoeVLPA scheme provides more accurate solutions than the first-order solutions.

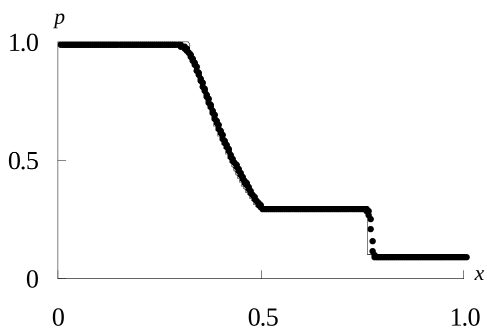

(a) *O*(1) of pressure

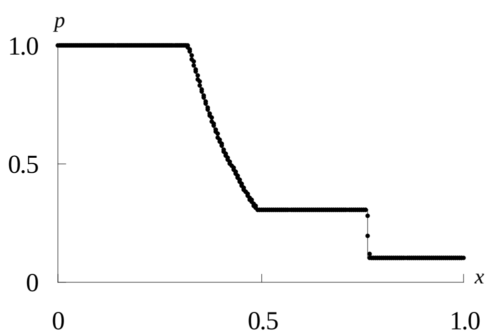

(b) *O*(2) of pressure

Figure 2: Comparison of exact and numerical solutions of pressure.

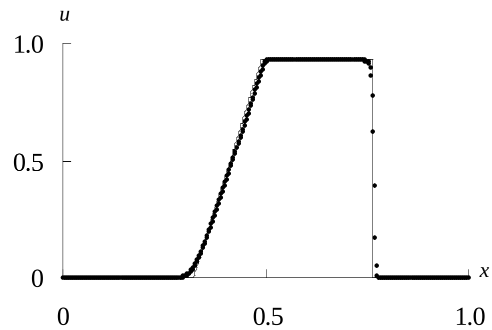

(a) *O*(1) of *x*-velocity

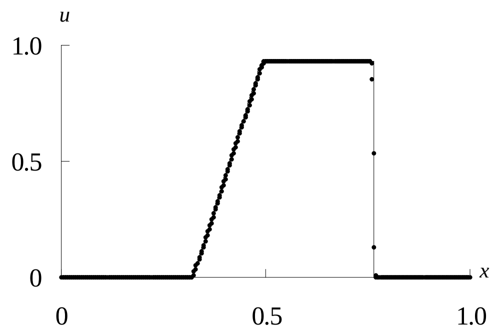

(b) *O*(2) of *x*-velocity

Figure 3: Comparison of exact and numerical solutions of *x*-velocity.

4.2 *Strong shock problem*

The one-dimensional strong shock problem [15] is simulated on a 1×0.1 domain, which discretized by uniform triangular elements (400×40). The initial conditions are given by $(\rho,u,p)_L = (1,0,1000)$ and $(\rho,u,p)_R = (1,0,0.01)$. Because of the very strong shock wave, the validity of the perfect gas equation of state may be questioned, but the purpose of using this test case is for numerical experiment to evaluate the different schemes. Another reason for choosing this problem is that the shock and the contact discontinuity are very closed to each other, within only about nine elements. It is thus very difficult for most of the numerical schemes to capture both the shock and the contact discontinuity within such a few elements. Figures 4(a)-(c) shows that the higher-order solutions of density, pressure, and *x*-velocity, respectively are improved but are still yielding oscillations slightly near the expansion fan and the contact discontinuity.

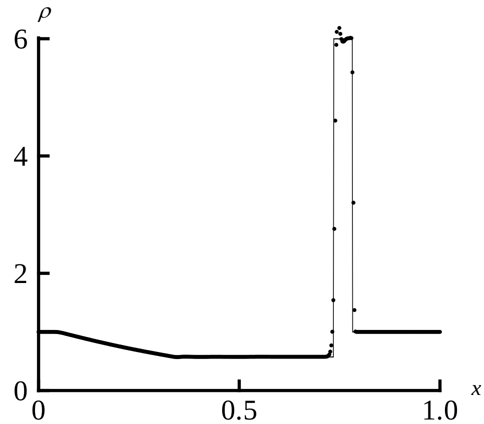

(a) $O(2)$ of density

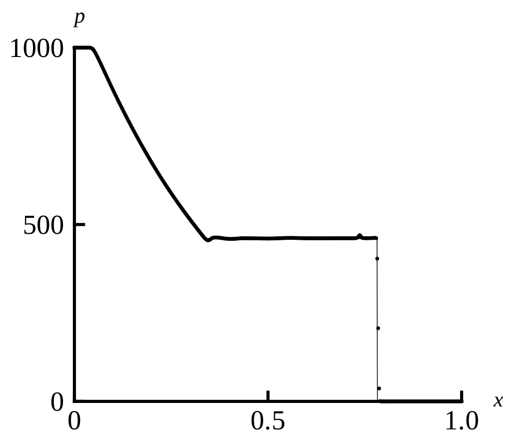

(b) $O(2)$ of pressure

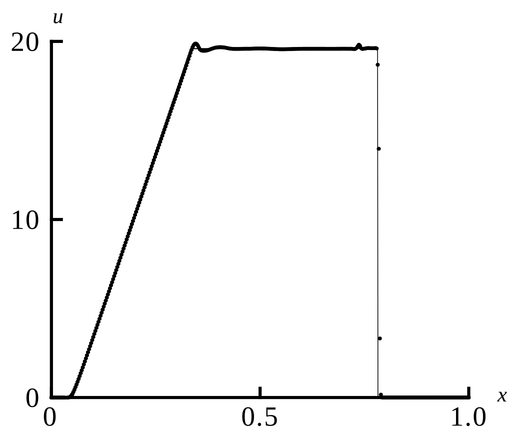

(c) $O(2)$ of x-velocity

Figure 4: Comparison of exact and numerical solutions of problem 4.2.

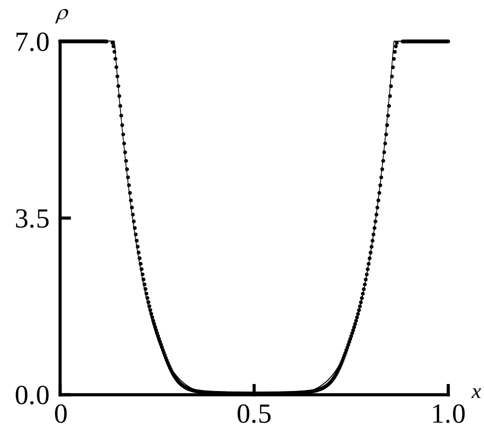

(a) $O(2)$ of density

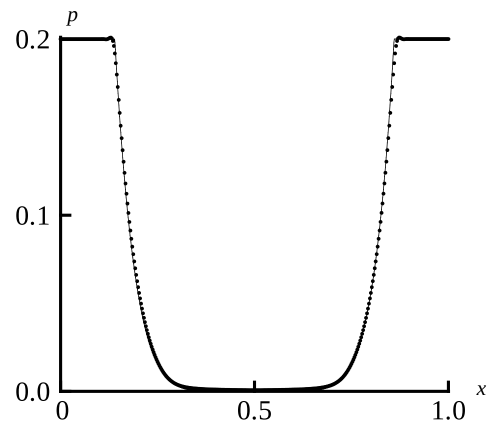

(b) $O(2)$ of pressure

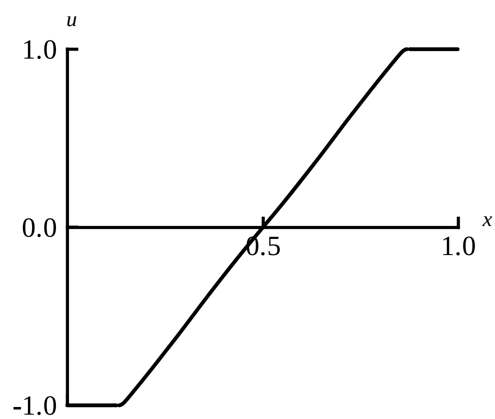

(c) $O(2)$ of x-velocity

Figure 5: Comparison of exact and numerical solutions of problem 4.3.

4.3 *Symmetric rarefaction wave*

The initial conditions of the symmetric rarefaction wave problem ($M = 5$) [16] are given by $(\rho, u, p)_L = (7, -1, 0.2)$ and $(\rho, u, p)_R = (7, 1, 0.2)$, such that they produce vacuum at the center of domain. Reference [9] shows that some numerical schemes cannot preserve the contact discontinuity. Figures 5(a)-(c) shows that the higher-order solutions of density, pressure, and *x*-velocity, respectively are preserve the contact discontinuity. The scheme produces a good approximation to the exact solution, and they noticeably small quantity of over-estimate the value of pressure in the middle of the expansion fan (at $x = 0.5$).

5 Conclusions

The present study demonstrates some important numerical challenges affecting the accuracy of shock tube problem on two-dimensional triangular grids. From a numerical point of view, the shock tube problem is a very interesting test case because the exact time-dependent solution is analytically known and can be compared with the computed solution by applying numerical approximations. A mixed entropy and shock fixes method is proposed to improve numerical stability of the Roe flux-difference splitting scheme (RoeVLPA). The method combines the modified fixes by Van Leer et al. and, Pandolfi and D'Ambrosio, together. The method was then evaluated by several well-known shock tube test cases and found to eliminate unphysical solutions that may arise from the use of the original Roe scheme. To further improve solution accuracy, the high-order spatial and second-order Runge-Kutta temporal discretization were also implemented. Computations were carried out based on the finite volume approach and instead of experimentation and the robustness of the numerical model and the accuracy of the simulations will be assessed through validation with the analytical ideal shock tube theory. The entire process was found to provide more accurate solutions for transient flow test cases.

Acknowledgments

The author is pleased to acknowledge the College of Industrial Technology, King Mongkut's University of Technology North Bangkok (KMUTNB), and the National Metal and Materials Technology Center (MTEC) for supporting this research work.

References

[1] Zucker R.D. and Biblarz O., 2002. *Fundamentals of Gas Dynamics*, 2nd edition, John Wiley & Sons, New Jersey.

[2] Perry K.M. and Imlay S.T., 1988. *Blunt-body Flow Simulations*, 24th AIAA/SAE/ASME/ASEE Joint Propulsion Conference, AIAA Paper-88-2904, Boston, MA.

[3] Quirk J.J., 1994. A Contribution to the Great Riemann Solver Debate, *International Journal for Numerical Methods in Fluid*, 18: 555-574.

[4] Roe P.L., 1981. Approximate Riemann solvers, parameter vectors, and difference schemes, *Journal of Computational Physics*, 43: 357-372.

[5] Pandolfi M. and D'Ambrosio D., 2001. Numerical Instabilities in Upwind Methods: Analysis and Cures for the "Carbuncle" Phenomenon, *Journal of Computational Physics*, 166: 271-301.

[6] Van Leer B., Lee W.T. and Powell K.G., 1989. *Sonic-Point Capturing*, AIAA 9th Computational Fluid Dynamics Conference, AIAA Paper-89-1945-CP, Buffalo, New York.

[7] Sanders R., Morano E. and Druguet M.C., 1998. Multidimensional Dissipation for Upwind Schemes: Stability and Applications to Gas Dynamics, *Journal of Computational Physics*, 145: 511-537.

[8] Phongthanapanich S. and Dechaumphai P., 2004. Flux-Difference Splitting Scheme with Modified Multidimensional Dissipation on Unstructured Meshes, *Journal of the Chinese Institute of Engineers*, 27: 981-992.

[9] Phongthanapanich S. and Dechaumphai P., 2009. Healing of Shock Instability for Roe's Flux-Difference Splitting Scheme on Triangular Meshes, *International Journal for Numerical Methods in Fluids*, 59: 559–575.

[10] Phongthanapanich S. and Dechaumphai P., 2004. Modified H-Correction Entropy Fix for Roe's Flux-Difference Splitting Scheme with Mesh Adaptation, *Transactions of the Canadian Society for Mechanical Engineering*, 28: 531-549.

[11] Frink N.T., Parikh P. and Pirzadeh S., 1991. *A Fast Upwind Solver for the Euler Equations on Three-Dimensional Unstructured Meshes, AIAA Paper-91-0102*, AIAA, 29th Aerospace Sciences Meeting and Exhibit, Reno, Nevada.

[12] Vekatakrishnan V., 1995. Convergence to Steady State Solutions of the Euler Equations on Unstructured Grids with Limiters, *Journal of Computational Physics*, 118: 120-130.

[13] Shu C.W. and Osher S., 1988. Efficient Implementation of Essentially Non-Oscillatory Shock-Capturing Schemes, *Journal of Computational Physics*, 77: 439-471.

[14] Sod G.A., 1978. A Survey of Several Finite Difference Methods for Systems of Nonlinear Hyperbolic Conservation Laws, *Journal of Computational Physics*, 27: 1-31.

[15] Toro EF., 1999. *Riemann Solvers and Numerical Methods for Fluid Dynamics*. Springer, Berlin.

[16] Linde T. and Roe P.L., 1997. Robust Euler Codes, 13th Computational Fluid Dynamics Conference, *AIAA Paper-97-2098*, Snowmass Village, CO.